COO-4094-89

CONF- 801102--23

Analytical Predictions of Liquid and Air Photovoltaic/Thermal Flat-Plate Collector Performance*+ ++

P. Raghuraman & S. D. Hendrie
Massachusetts Institute of Technology
Lincoln Laboratory
Lexington, Massachusetts 02173

MASTER

ABSTRACT

Two separate one-dimensional analyses have been developed for the prediction of the thermal and electrical performance of both liquid and air flat-plate photovoltaic/thermal (PV/T) collectors. The analyses account for the temperature difference between the primary insolation absorber (the photovoltaic cells) and the secondary absorber (a thermal absorber flat plate). The results of the analyses are compared with test measurements, and therefrom, design recommendations are made to maximize the total energy extracted from the collectors.

NOMENCLATURE

A_c	Cell Envelope Area, cm^2
A_t	Gross Collector Area, cm^2
C_p	Specific Heat of Working Fluid, J/kg°k
D	Outer Diameter of Tubes in Liquid Collector, cm
D_i	Inner Diameter of Tubes in Liquid Collector, cm
d	Air Gap Height Below Top Glass Cover, cm
d_a	Air Channel Height in Air Collector, cm
d_p	Thickness of Pottant in Liquid Collector, cm
d_r	Thermal Absorber-Plate Thickness, cm
E_c	Insolation Absorbed by the Photovoltaic Cells, w/cm^2
E	Energy Loss Flux From Collector, w/cm^2
E_r	Insolation Absorbed by Thermal Absorber Plate, w/cm^2
E_{ca}	Radiant Energy Flux to Thermal Absorber Plate From Photovoltaic Cells, w/cm^2
E_{ce}	Electrical Energy Produced by Photovoltaic Cells, w/cm^2
E_{cr}	Heat Conducted From Photovoltaic Cells to Thermal Absorber Plate, w/cm^2
E_{ct}	Thermal Energy Released by Photovoltaic Cells, w/cm^2
F	Collector Fin Efficiency
F'	Collector Efficiency Factor
h_c	Cell-Glass Composite Heat-Transfer Coefficient in Air Collector, w/cm^2°C
h_g	Top Glass Cover Heat-Transfer Coefficient, w/cm^2°C
h_i	Heat-Transfer Coefficient between Tube Wall and Liquid in Liquid Collector, w/cm^2°C
h_r	Absorber-Plate Heat-Transfer Coefficient in Air Collector, w/cm^2°C
h_{cg}	Air-Gap Heat-Transfer Coefficient, w/cm^2°C
I	Insolation, w/cm^2
K_a	Thermal Conductivity of Air, w/cm°C
K_p	Thermal Conductivity of Pottant, w/cm°C
K_r	Thermal Conductivity of Absorber Plate, w/cm°C
ℓ	Cell Envelope Length, cm
$\dot{m}$	Total Mass Flow Rate of Working Fluid Through Collector, kg/s
p	Cell Packing Factor, Defined as Ratio of Total Cell Area to Cell Envelope Area
Q	Total Collector Heat-Transfer Rate to Working Fluid, w

---

*This work was sponsored by the U.S. Department of Energy.

+To be presented at the ASME Winter Annual Meeting, Chicago, Illinois, 16-21 November 1980.

++The U.S. Government assumes no responsibility for the information presented.

Q_c	Total Cell-Glass Composite Heat-Transfer Rate to Air Flow, w
Q_r	Total Absorber-Plate Heat-Transfer Rate to Air Flow, w
q_c	Cell-Glass Composite Heat-Transfer Rate to Air Flow, per Unit Cell Envelope Area, w/cm^2
q_r	Absorber-Plate Heat-Transfer Rate to Air Flow, per Unit Cell Envelope Area, w/cm^2
Ra	Air-Gap Rayleigh Number
T_f	Local Fluid Temperature, °K
T_{fi}	Inlet Fluid Temperature, °K
T_{fo}	Outlet Fluid Temperature, °K
T_o	Reference Temperature at which Cell Efficiency η_o is defined, °K
$\bar{T}_c$	Average Cell Temperature, °K
$\bar{T}_g$	Average Front-Glass Temperature, °K
$\bar{T}_r$	Average Absorber-Plate Temperature, °K
U_L	Collector Loss Coefficient, $w/cm^2 {}^\circ K$
V	Wind Velocity, m/s
w	Center-to-Center Spacing between Tubes in Liquid Collector, cm
W	Cell Envelope Width, cm
α_c	Cell Absorptance to Visible Light
α_r	Thermal Absorber-Plate Absorptance to Visible Light
α_{cI}	Cell Absorptance to Infrared Light
α_{gI}	Glass Absorptance to Infrared Light
α_{rI}	Absorber-Plate Absorptance to Infrared Light
β	A Constant ranging from 0 to 1. Used to indicate Effective Decrease in Cell-Glass Heat-Transfer Area to Air Flow
Δ	Change in Cell Efficiency per Unit Cell Temperature Change, ${}^\circ K^{-1}$
ϵ_c	Cell Emissivity in Infrared Range
ϵ_g	Glass Emissivity in Infrared Range
ϵ_r	Absorber-Plate Emissivity in Infrared Range
η_e	Single-Cell Efficiency with Encapsulation
η_{elec}	Electrical Efficiency of Collector
η_{therm}	Thermal Efficiency of Collector
η_o	Reference Cell Efficiency at Temperature T_o.
θ	Collector Inclination
σ	Stefan-Boltzmann Constant, $w/cm^2 {}^\circ K^4$
τ_g	Glass Transmissivity to Visible Light (one and two glasses for liquid and air collector, respectively)
τ_p	Transmissivity of Pottant to Visible Light

INTRODUCTION

Combined photovoltaic/thermal (PV/T) flat-plate collectors provide an attractive alternative to units that collect either thermal or electrical energy, especially when space limitations and installation costs are of primary concern. A conceptual design study[1] of combined PV/T collector heat-pump solar systems for a single-family residence shows that they can be economically competitive in cold climates such as the northeastern and northcentral regions of the U. S. Numerical methods predicting the thermal and electrical performances of two typical PV/T collector designs, one liquid and the other air, are described here. Such PV/T collectors have been the subject of considerable study at MIT Lincoln Laboratory. The analyses use heat-transfer properties--radiative, conductive and convective--for each collector component, thereby facilitating the study of collector constitutents and their influence on collector performance.

Fig. 1 depicts a cross section of the liquid PV/T collector. It includes a top glass cover separated from the photovoltaic (PV) cells by an air space. The cells, which are the primary absorber of insolation, are separated from the secondary absorber, a painted aluminum plate, by a layer of electrical insulation. Tubes attached to the back of the thermal absorber carry the working fluid. Thermal insulation on the side and the back of the PV/T collector keeps heat losses small. Fig. 2 depicts a cross section of the air PV/T collector. It consists of two glass covers with photovoltaic cells mounted on the underside of the inner glass cover. The cells are again the primary absorber of the incident insolation. A black-painted aluminum thermal absorber plate placed below the air-flow channel receives insolation passing between the cells. Again, a sufficient amount of insulation on the side and back of the PV/T collector keeps heat losses small.

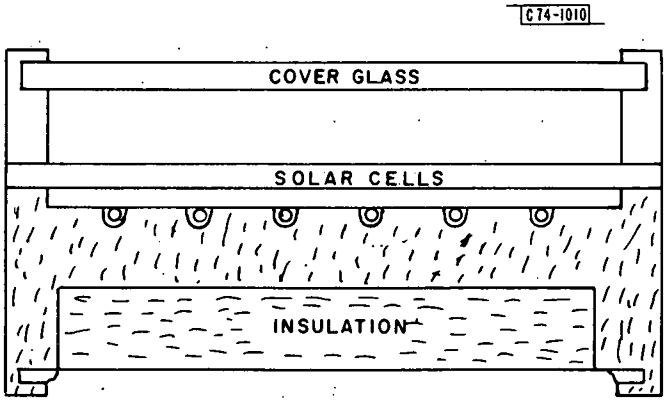

FIG. 1: LIQUID PV/T COLLECTOR

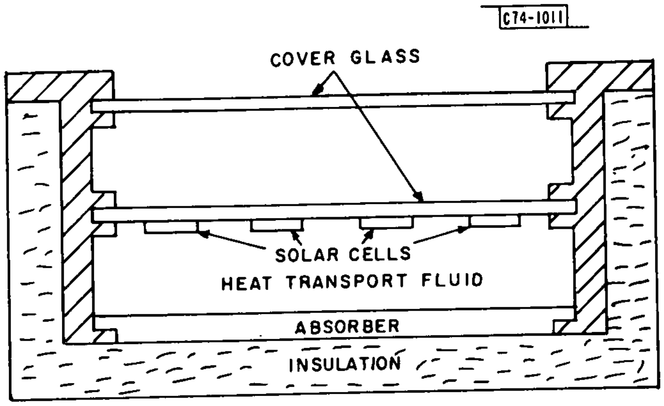

FIG. 2: AIR PV/T COLLECTOR

Test measurements on such liquid and air PV/T collectors have been made by Biringer, et al[2], at Sandia Laboratories and Hendrie,[3,4] at MIT Lincoln Laboratory. Analytical solutions to thermal collector performance available from the classical analysis of Hottel and Whillier[5] have been extended to these PV/T collectors by Florschuetz[6]. A key feature of the Florschuetz analysis is the modeling of the photovoltaic cells and absorber plate as a composite with uniform temperature. However, following the test measurements of Hendrie[4], there appears to be a considerable temperature difference between the PV cells and the thermal absorber, about 12°C for liquid and 8°C for air PV/T collectors. For the liquid PV/T collector, this temperature differential is attributable to the large, thermal resistance provided by the currently used electrical insulation, silicone pottant (thermal conductivity, 0.002 watts/cm°C; thickness ≈ 0.5 cm), between the PV cells and the thermal absorber. For the air collector, this differential results from an undulated cell-glass surface[4] having a much lower heat-transfer coefficient to the air flow in the channel than a smoother thermal absorber surface. It is speculated that these large undulations on the cell surface create large recirculation regions on the cell-glass surface, resulting in very poor heat transfer from the cell to the air flow. In fact, Florschuetz's analysis overestimates by more than 10% the thermal performance data of Hendrie, for both liquid and air PV/T collectors.

The analyses described herein--extending Florschuetz's analysis and predicting test measurements more closely--account for the PV cell to absorber-plate-temperature difference. The next section describes the model and the relevant equations used. The last section compares the result of the analyses with test measurements, and therefrom, draws some conclusions on the design of PV/T collectors.

FORMULATION AND ASSUMPTION OF MODEL

The analytical model used for both air and liquid PV/T collectors closely follows the thermal model of Hottel[5]. Edge and back heat losses are neglected and the heat transfer in the collector is envisioned as the sum total of several one-dimensional heat-transfer processes--three for the liquid and two for the air collector. These include the one-dimensional heat transfer through the front glass cover to the primary and secondary absorber, fin heat transfer between the tubes (only for the liquid collector), and the heat transfer to the working fluid from the collector surface(s) in contact with it. At the outset, the energy conservation equation is applied to each collector component per unit cell envelope area to yield a system of algebraic equations for the average temperature of each collector component and the heat transfer to the working fluid from the enveloping surface(s). The Hottel fin model is then used to calculate the fin heat transfer between tubes for the liquid collector. The heat transfer to the working fluid from the collector surfaces enveloping the fluid is then calculated assuming that each of these surfaces is at a constant temperature, i.e., neglecting heat conduction on these surfaces in a direction opposite to that of the fluid flow.

Neglecting inter-reflection of insolation between the various surfaces and absorption by the glass surfaces, the net energy absorbed by the cell per unit cell envelope area is

$$E_c = p\alpha_c\tau_g I,$$

where I = the insolation incident on the glass cover,

τ_g = fraction transmitted through the front glass cover (and second glass surface for the air collector) to the cell,

α_c = cell absorptivity to visible light,

and p = cell packing factor defined as the fraction of the cell envelope area occupied by the cells.

Insolation incident between cells is transmitted through the pottant and absorbed by the thermal absorber. Again, neglecting inter-reflection of insolation between the cell and the thermal absorber, the energy per unit area absorbed by the thermal absorber is

$$E_r = (1-p)\,\tau_g\tau_p\alpha_r I,$$

where α_r = the absorptivity of the thermal plate to visible light,

and τ_p = transmittance of the pottant.

From the insolation absorbed by the cell, the electrical and thermal energy per unit cell envelope area produced by it are, respectively,

$$E_{ce} = \eta_e p\,\tau_g I,$$

and $$E_{ct} = (1-\eta_e/\alpha_c)\,p\alpha_c\tau_g I,$$

where η_e is the cell electrical efficiency.

Neglecting temperature gradients in the glass surfaces of both liquid and air collectors, let $\bar{T}_c$, $\bar{T}_r$ and $\bar{T}_g$ be the average cell, absorber plate and glass temperatures. The thermal energy released by the cell is then partly lost to the top cover glass by a combination of natural convection and/or conduction through the air gap and radiation interchange between the surface facing the top glass cover across the air gap and the top glass cover. This loss to the cover glass is given by,

$$E_\ell = h_{cg}(\bar{T}_c - \bar{T}_g) + \alpha_{gI}\,\epsilon_f\,\sigma\bar{T}_c^4 - \alpha_f\,\epsilon_g\,\sigma\bar{T}_g^4$$

where h_{cg} = the convective heat-transfer coefficient in the air gap,

σ = Stefan-Boltzman constant,

α_{gI} = glass absorptivity (infrared region),

ϵ_g = glass emissivity,

α_f = absorptivity (infrared) of the surface facing the top glass cover across the air gap (glass and cell for the air and liquid collector, respectively),

and ϵ_f = emissivity of the surface facing the top glass cover.

Here absorption of infrared radiation by the air gap is neglected as is inter-reflection of infrared radiation across the air gap. For small air gap thickness d, the heat transfer in the air gap is purely conductive; with increasing values of d, natural convection in the air gap becomes the dominating heat-transfer mode. Following Buchberg, et al[7], h_{cg} is given as:

$$\frac{h_{cg}d}{K_a} = 0.157\ \mathrm{Ra}^{0.285}, \quad \text{for Ra} > 2 \times 10^4$$

and

$$\frac{h_{cg}d}{K_a} = 1 \quad \text{for Ra} < 1.7 \times 10^3$$

where K_a = the thermal conductivity of air

and Ra = the Rayleigh number based on d.

This heat loss is transferred by the top glass cover to the ambient air by a combination of natural and forced convective heat transfer and radiant heat exchange with the sky. It is given by

$$E_\ell = h_g(\bar{T}_g - T_a) + \epsilon_g\,\sigma\bar{T}_g^4 - \alpha_{gI}\,\sigma(T_a - 3)^4$$

where T_a = the ambient temperature and T_a - 3°C is assumed to be the sky temperature,

and h_g = the convective heat-transfer coefficient of the glass surface.

Following Stultz and Wen[8], h_g is available as:

$$h_g = \left[1.247\ (\bar{T}_g - T_a)\cos\theta\right]^{1/3} + 2.658V,$$

where h_g has the unit, watts/m^2°K; the temperatures are in °C,

V = the wind velocity in m/sec,

and θ = the module inclination to the horizontal.

The balance of the thermal energy released by the cell that is not lost through the front glass cover is transferred to the thermal absorber plate and working fluid. For the liquid collector, the pottant between the cells and the absorber plate is opaque to infrared radiation and heat is transferred from the cells to the absorber plate by conduction alone.

It is given as:

$$E_{cr} = \frac{K_p}{d_p}(\bar{T}_c - \bar{T}_r)$$

where d_p = thickness of pottant,

and K_p = thermal conductivity of pottant.

For the air collector, the balance of the thermal energy released by the cell which is not lost through the front glass cover is partly convected away by the air flow, q_r (per unit cell envelope area), while the rest is radiated to the absorber plate:

$$E_{ca} = \alpha_{rI}\,\epsilon_c\ \bar{T}_c^4 - \alpha_{cI}\,\epsilon_r\ \bar{T}_r^4,$$

where α_{rI} = infrared absorptance of the absorber plate,

α_{cI} = infrared absorptance of the cell-glass composite,

ϵ_r = emittance of the absorber plate,

and ϵ_c = emittance of the cell-glass composite.

Here we have neglected inter-reflection of radiation between the absorber and the cell-glass face, as well as absorption of any radiation by the air flow. The absorber plate loses heat by convection, q_r (per unit cell envelope area), to the air flow. An application of the energy conservation law to each collector component per unit cell envelope area yields the following set of equations for the liquid collector:

$$(1 - \eta_e/\alpha_c)\ p\,\alpha_c\tau_g I = \alpha_{gI}\,\epsilon_c\,\sigma\bar{T}_c^4 - \alpha_{cI}\,\epsilon_g\,\sigma\bar{T}_g^4 + h_c\left(\bar{T}_c - \bar{T}_g\right) + \frac{K_p}{d_p}(\bar{T}_c - \bar{T}_r), \tag{1}$$

$$\epsilon_g\,\sigma\bar{T}_g^4 - \alpha_{gI}\,\sigma(T_a - 3)^4 + h_g(\bar{T}_g - T_a) = (1 - \eta_e/\alpha_c)\ p\,\alpha_c\,\tau_g I - \frac{K_p}{d_p}(\bar{T}_c - \bar{T}_r). \tag{2}$$

The corresponding set for the air collector is

$$(1 - \eta_e/\alpha_c)\ p\,\alpha_c\tau_g I = \alpha_{gI}\,\epsilon_g\,\sigma(\bar{T}_c^4 - \bar{T}_g^4) + h_c(\bar{T}_c - \bar{T}_g) + q_c + \alpha_{rI}\,\epsilon_c\,\sigma\bar{T}_c^4 - \alpha_{cI}\epsilon_r\,\sigma\bar{T}_r^4, \tag{3}$$

$$\epsilon_g\,\sigma\bar{T}_g^4 - \alpha_{gI}\,\sigma(T_a - 3)^4 + h_g(\bar{T}_g - T_a) = \alpha_{gI}\ \epsilon_g\,\sigma(\bar{T}_c^4 - \bar{T}_g^4) + h_c(\bar{T}_c - \bar{T}_g), \tag{4}$$

and

$$(1-p)\ \tau_g \tau_p \alpha_r I + \alpha_{rI}\ \epsilon_c \sigma \bar{T}_c^{\ 4} - \alpha_{cI}\ \epsilon_r\ \sigma \bar{T}_r^{\ 4} = q_r . \quad (5)$$

The cell electrical efficiency, η_e, in equations (1) and (3) is modeled by a linear relation,

$$\eta_e = \eta_o \left[1 - \Delta\left(\bar{T}_c - T_o\right)\right], \quad (6)$$

where η_o, Δ and T_o are constants.

Besides equations (1) and (2) for the liquid collector, an additional equation is obtained by considering the fin heat transfer between tubes and the heat transferred to the tubes along the flow length. Following Hottel and Whillier[5] (see also Duffie and Beckman,[9]), the heat transfer by tubes to the fluid at local temperature T_f is given as

$$Q = wF' \left[(1-p)\ I\ \tau_g\ \tau_p \alpha_r + \frac{K_p}{d_p}\left(\bar{T}_c - T_f\right)\right], \quad (7)$$

with

$$wF' = \frac{\dfrac{d_p}{K_p}}{\left[\dfrac{K_p}{d_p}(D+F)\right]^{-1} + \left(\pi D_i h_i\right)^{-1}}$$

and

$$F = 2\sqrt{\frac{d_p K_r d_r}{K_p}}\ \mathrm{Tanh}\left[\sqrt{\frac{K_p}{d_p K_r d_r}}\left(\frac{w-D}{2}\right)\right],$$

where

w = The center-to-center distance between tubes of inner and outer diameter, D_i and D,

h_i = the heat-transfer coefficient between the fluid and the tube wall,

and

K_r = the thermal conductivity of the plate of thickness, d_r.

It has been assumed here that the bond conductance between the tube and the absorber plate is infinite. Equating (7) to the useful heat gain by the fluid in the tube per unit flow length[9], and integrating the resulting equation over the entire collector length, ℓ, the total heat transferred to the fluid in terms of incoming fluid temperature, T_{fi}, is

$$Q = \frac{\dot{m} C_p d_p}{K_p}\left(1 - \exp\left[\frac{-K_p F' A_c}{d_p \dot{m} C_p}\right]\right) \left[(1-p)\ I\ \tau_g\ \tau_p\ \alpha_r + \frac{K_p}{d_p}\left(\bar{T}_c - T_{fi}\right)\right], \quad (8)$$

where

$\dot{m}$ = the total mass flow rate through the collector,

C_p = specific heat of the liquid,

and

A_c = cell envelope area ℓW.

However, the total heat transfer to the fluid is also given as,

$$Q = A_c\left[\frac{K_p}{d_p}\left(\bar{T}_c - \bar{T}_r\right) + (1-p)\ I\ \tau_g\ \tau_p\ \alpha_r\right]. \quad (9)$$

Equating (8) and (9) provides the additional relation between $\bar{T}_c$ and $\bar{T}_r$.

For the air collector the flow passage is a channel and so there is no fin heat transfer. Proceeding as for the liquid collector, the total useful heat gain by the air flow, $Q = A_c\ (q_c + q_r)$, is obtained as:

$$Q_d = q_d A_c = A_c h_d \left[\bar{T}_d - \frac{(h_c\bar{T}_c + h_r\bar{T}_r)}{h_c + h_r} - \frac{\dot{m} C_p}{(h_c + h_r)\ \ell W} \left\{T_{fi} - \frac{(h_c\bar{T}_c + h_r\bar{T}_r)}{h_c + h_r}\right\} e^{\left[\frac{-\ell W(h_c + h_r)}{\dot{m} C_p}\right]}\right],$$

$$d = c,\ r, \quad (10)$$

where

h_c = the heat-transfer coefficient of the cell-glass composite,

h_r = heat-transfer coefficient of the absorber-plate surface,

ℓ = cell envelope length

and W = cell envelope width,

with A_c = ℓW.

Following Kays[10], where the value for the Nusselt number for fully developed laminar velocity and temperature profiles between parallel plates is tabulated, we assume that h_r and h_c are given by,

$$\frac{2h_r d_a}{K_a} = \frac{2h_c d_a}{K_a} = 7.54$$

where d_a = height of the air channel.

Thus equations (1), (2) and (8-9) provide 3 equations in 3 unknowns $\bar{T}_c$, $\bar{T}_g$, and $\bar{T}_r$ for the liquid collector while (3), (4), (5) and (10) provide 5 equations for 5 unknowns $\bar{T}_c$, $\bar{T}_g$, $\bar{T}_r$, Q_c, and Q_r. Solutions to each set of equations were obtained on the computer using a Newton-Raphson iteration technique. The procedure used was to assume a cell temperature, calculate all the other unknowns and finally the cell temperature. If the calculated cell temperature yields the same value as the assumed temperature, the solution has converged. Typically, the solution converged in about 6 iterations. From the solutions, the collector thermal and electrical efficiencies, η_{therm} and η_{elec}, are obtained as

$$\eta_{therm} = \frac{Q}{IA_t}$$

and $$\eta_{elec} = \frac{\eta_e p A_c}{A_t} \tau_g$$

where A_t is the gross collector area.

RESULTS

The analyses were used to examine the electrical and thermal performance of the liquid and air PV/T collectors tested at MIT Lincoln Laboratory[3,4] under ASHRAE 93-77 standards. Table I shows a listing of the various parameters of the PV/T systems used; namely geometry, thermal and flow properties. The mass flow rate for the air collector was 0.0186 kg/sec, while for the liquid collector, where propylene glycol (C_p = 2.47 kJ/kg°C) was the working fluid, a mass flow rate of 0.035 kg/sec was used. Calculations were done for wind velocity of 2.2 m/sec and module inclination, 55°. Figs. 3 and 4 show the analytical results for η_{therm}, the thermal efficiency for the liquid and air collectors, respectively, for collector operation with concurrent electrical energy collection from the PV cells. As done for conventional solar thermal collectors, η_{therm} is plotted as a function of $\frac{T_{fi} - T_a}{I}$. The method used to generate the efficiency curves was to vary T_{fi}, keeping I = 1 kW/m^2, T_a = 295°K. For the liquid collector, due to problems of accessibility, the silicone pottant thickness (thermal conductivity, K_p = 0.002 Watts/cm°C) could only be estimated[4] to be between 1 to 5 mm and so calculations were done for both d_p = 1 mm and 5 mm. For the air collector, a visual examination was made (using photographs) of the cell-pottant surface. It revealed an excessive application of pottant around the cell circumference causing formation of large ridges on the cell back surface. Further, with the cells affixed to the glass surface, the cell presents a series of steps past which circulating air flows. The flow recirculates in these step-like regions, reducing the heat transfer from the cells and the glass. This reduced heat transfer is accounted for by scaling down the heat-transfer coefficient, $2h_c = 7.54 \frac{K_a}{d_a}$, by a factor β, where β is a constant whose value lies between 0 and 1. Calculations for the air collector were done for β = 0.5 and, for comparison, β = 1.

Fig. 3 shows that for the liquid collector the thermal efficiency curve generated from the analysis matches test data satisfactorily for a pottant thickness, d_p, of 5 mm. For d_p = 1 mm, the analysis overpredicts the values of η_{therm} over test data, even though the slope of the two curves, a measure of the collector loss coefficient, U_L, is relatively unaffected. From the analysis, it appears that the thermal efficiency of the liquid collector decreases by about 2% for every mm increase in the silicone pottant thickness with the loss coefficient, U_L, being almost a constant. Table II compares the computed heat-transfer coefficients between various collector surfaces. Not unexpectedly, the value of U_L is close to values for corresponding solar thermal collectors.

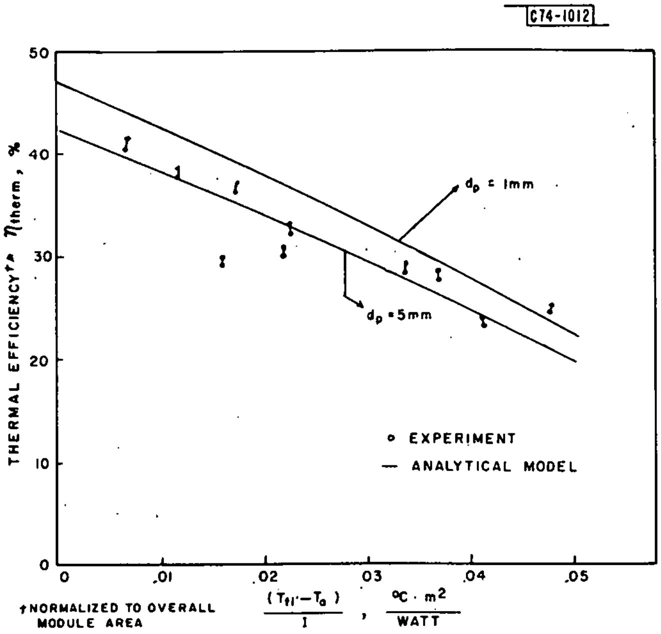

† NORMALIZED TO OVERALL MODULE AREA
* PROPYLENE GLYCOL

FIG. 3 LIQUID PV/T COLLECTOR THERMAL EFFICIENCY WITH ELECTRICAL ENERGY COLLECTION

Fig. 4 for the air collector shows that the results of the analysis match test data satisfactorily for β = 0.5. When β = 1, the thermal efficiency increases by about 10%, without affecting U_L. This then represents the thermal gain by ensuring the entire cell-glass composite transfers heat to the air flow. The air PV/T heat-transfer coefficients computed from the analysis and test data for this collector are shown in Table II.

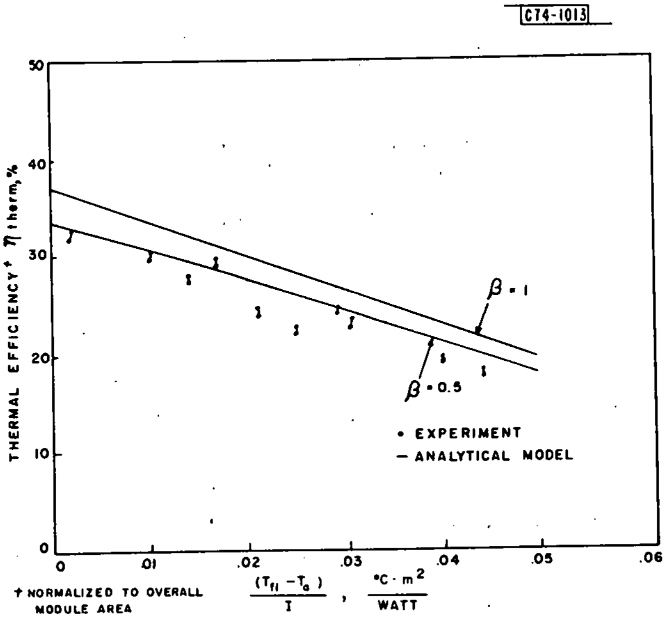

† NORMALIZED TO OVERALL MODULE AREA

FIG. 4 : AIR PV/T COLLECTOR THERMAL EFFICIENCY WITH ELECTRICAL ENERGY COLLECTION

Fig. 5 shows the air ($\beta = 0.5$) and liquid (d_p = 5 mm) collector electrical efficiencies, η_{elec}, computed from experiment and analysis, plotted as a function of average fluid temperature in the collector, $\frac{T_{fo} + T_{fi}}{2}$. The analyses again compare well with test measurements. We note that η_{elec} varies with respect to its value at the cell reference temperature by less than 17% over the range of 0 to 50°C for $(T_{fi} + T_{fo})/2$. This variation depends on the value of Δ, the change in cell efficiency with cell temperature. Following Hovel[12], for typical cell efficiencies of 12% at room temperature, Δ varies between 0.0033 to 0.005 for conventional silicon cells with 1-10 ohm-cm resistivities. Therefrom, 17% represents a typical upper bound to cell electrical efficiency changes for $(T_{fo} + T_{fi})/2$ variations from 0 to 50°C.

C74-1016

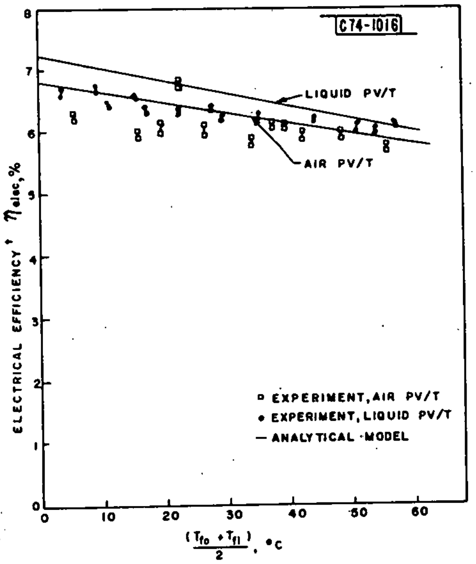

†NORMALIZED TO OVERALL COLLECTOR AREA

FIG. 5: ELECTRICAL EFFICIENCY vs AVERAGE FLUID TEMPERATURE

C74-1015

TABLE I

PV/T COLLECTOR COMPONENT PARAMETERS

Parameter	Liquid PV/T Collector	Air PV/T Collector
Cell Envelope / Total Collector Area	0.82	0.81
Length x Width	190 cm x 84 cm	149 cm x 85 cm
Packing Factor	0.91	0.78
Cell Constants		
η_o	0.108	0.118
T_o	301° K	318 ° K
Δ	.0042° K^{-1}	.0036° K^{-1}
Tube Diameters		
D	1.59 cm	----
D_i	1.27 cm	----
Air Gap Height	1.27 cm	1.27 cm
Absorber Plate Thickness	0.08 cm	----
Air Flow Channel Height	----	0.71 cm
Glass Transmittance	0.89	0.88
Pottant Transmittance	0.85	0.85
Absorptance (visible, infrared), Emittance		
Cell:		
α_c	0.895	0.89
α_{cI}	0.92	0.87
ϵ_c	0.86	0.92
Glass:		
α_g	0	0
α_{gI}	1.0	1.0
ϵ_g	0.86	0.87
Absorber Plate:		
α_r	0.9	0.88
α_{rI}	---	0.87
ϵ_r	---	0.87

C74-1014

TABLE II

COMPUTED HEAT-TRANSFER COEFFICIENTS + *

	Experimental	Analysis
Air PV/T Collector		
U_L	7.2	6.2
Collector Heat Removal Factor	0.57	0.54
$\overline{\tau\alpha}$	0.60	0.61
h_c	6.12	6.0
Liquid PV/T Collector		
U_L	6.77	6.9
Collector Heat Removal Factor	0.65	0.65
$\overline{\tau\alpha}$	0.68	0.65
K_p/d_p	24.9	40.

+ In watts/m^2°C

* Based on Gross Collector Area

CONCLUSIONS AND RECOMMENDATIONS

Analyses have been developed for liquid and air PV/T collectors that compare well with available test data. From results of the analyses, it appears that the thermal performance of currently available collectors can be improved markedly by the following modifications to existing PV/T collector designs:

(i) Heat losses through the top cover glass to the ambient air typically are made up of 60% radiative and 40% convective losses. Convective losses may be reduced, it is conjectured, by a series of crisscrossing grooves on the top glass cover. These grooves aid in the formation of recirculation zones in the ambient air flowing over the surface and therefore reduce the effective convective heat-transfer coefficient of the glass surface.

(ii) The limited data of Buchberg, et al, suggests that there exists an optimum, cell-to-glass-cover air-gap height for which the thermal conductance to heat loss is a minimum. This height is critically dependent on the cell-to-glass temperature difference. For the calculated temperature difference of 8 to 17°C, corresponding to insolation values between 50 to 100 mw/cm^2, this height should be greater than 5 cm as opposed to 1.27 cm in current designs. This change is expected to reduce top losses. However, care has to be taken to prevent shadowing of the photovoltaic cells.

(iii) The thermal resistance between the cells and the working fluid must be kept as small as possible. For the liquid collector this thermal resistance is represented by the electrical insulation between the cells and the absorber plate, while for the air collector it is the epoxy applied at the back of the cell insulating it from the air flow. In both cases, the traditional insulation used is silicone pottant, which has a thermal conductivity, K, of 0.0002 watts/cm°C. However, several high thermal conductivity, high di-electric strength epoxies are available with values of K ranging from 0.0008 to 0.016 watts/cm°C. Use of these epoxies in place of the silicone pottant, would ensure a low thermal resistance between the cells and the thermal collector while ensuring electrical isolation.

(iv) For the air collector, elimination of large step-like undulations on the cell-glass surface normal to the flow direction will prevent recirculating flow regions.

(v) For the liquid collector, heat resistance resulting from air gaps between the absorber plate and the liquid-carrying tubes can be minimized by making the tubes an integral part of the absorber plate. One such commercially available absorber-plate design is referred to as a "Roll Bond"* absorber plate. A rectangular section for these tubes with a width-to-height ratio greater than 3, has a higher heat-transfer coefficient than a circular tube. The larger this ratio, the higher the heat-transfer coefficient.

(vi) In both the liquid and air PV/T collector designs, the flow is laminar. Higher heat-transfer coefficients would result if the flow were turbulent. This would be difficult to do for liquid collectors as the relevant Reynolds number is not high enough either to cause or maintain turbulence in the flow. However, for air collectors this is possible, for example, by placing trip wires on the channel walls normal to the flow. For both air and liquid collectors, even without making the fluid turbulent, increased heat transfer can be obtained by making the tube and channel walls rough and also by placing fins along the flow directions.

(vii) The use of anti-reflective coatings on the surfaces of the glass cover(s) would substantially reduce reflection of insolation. Two examples of these coatings are made with magnesium fluoride and bismuth oxide.

(viii) The use of selective black coatings of black nickel or chrome on the thermal collector plate should increase the thermal efficiency of collector and lower the collector loss coefficient. These coatings are almost perfect absorbers of insolation and have a very low emissivity.

In deciding their relative merit, the effectiveness of some of these measures has to be weighed against the penalties they entail--for example, measures (v) and (vi) lead to increased pump costs, while measures (vii) and (viii) add considerably to the initial system costs.

PV/T collectors currently use conventional photovoltaic cells that are ideal for photovoltaic modules producing electrical power only. Work is underway at Lincoln Laboratory by Cox[11] to tailor these PV cells for application to PV/T collectors. It is anticipated that such changes in current designs will substantially improve the performance of PV/T collectors.

REFERENCES

1. M. C. Russell, "Solar Photovoltaic/Thermal Residential Systems," COO 4577-9, Massachusetts Institute of Technology, Lincoln Laboratory, Lexington, Massachusetts (1979).
2. K. L. Biringer and D. R. Smith, "Development and Testing of Combined Photovoltaic/Thermal Flat-Plate Collectors," 1978 meeting of the American Section of the International Solar Energy Society.
3. S. D. Hendrie, "Evaluation of Combined Photovoltaic/Thermal Collectors," International Solar Energy Society, 1979 International Congress, Atlanta, Georgia, 28 May-1 June 1979.
4. S. D. Hendrie and P. Raghuraman, "A Comparison of Theory and Experiment for Photovoltaic/Thermal Collector Performance," Proc. of the 14th IEEE Photovoltaic Specialists' Conference, San Diego, California, 7-10 January 1980.
5. H. C. Hottel and A. Whillier, "Evaluation of Flat-Plate Solar Collector Performance," Transactions of the Conference on the Use of Solar Energy, The Scientific Basis, Volume II, Part 1, Section A, 74-104, University of Arizona Press, Tucson, Arizona, 1958.
6. L. W. Florschuetz, "Extension of the Hottel-Whillier Model to the Analysis of Combined Photovoltaic/Thermal Flat-Plate Collectors," Solar Energy, Volume 22, 1979, pp. 361-366.
7. H. Buchberg, I. Catton and D. K. Edwards, "Natural Convection in Enclosed Spaces; A Review of Application to Solar Energy Applications," ASME paper 74-WA/HT-12, New York 1974.
8. J. W. Stultz and L. C. Wen, "Thermal Performance Testing and Analysis of Photovoltaic Modules in Natural Sunlight," LSSA Project Task Report 5101-31, Jet Propulsion Laboratory, California Institute of Technology, Pasadena, California, 29 July, 1977.
9. J. A. Duffie and W. A. Beckman, Solar Energy Thermal Processes, Wiley, New York (1974) p. 138-147.
10. W. M. Kays, Convective Heat and Mass Transfer, McGraw-Hill Book Company, New York (1960), p. 117.
11. C. H. Cox, "Optimization of Photovoltaic Cells for Use in Combined Phototoltaic/Thermal Collectors," Presented at the ASME Winter Meeting, Chicago, Illinois, 16-21 November 1980.
12. H. J. Hovel, Semiconductors and Semimetals, Volume II, Solar Cells, Academic Press, New York 1975, p. 173.

---

* Ⓡ Olin Brass Corporation